

FOR REFERENCE

NOT TO BE TAKEN FROM THIS ROOM

FATIGUE CRACK INITIATION IN 2024-T3 ALUMINIUM ALLOY

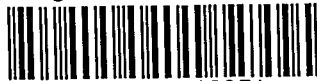
by

ALI SARIMUSTAFA

Submitted to the faculty of the engineering
in partial fulfillment of the requirements
for the degree of

MASTER OF SCIENCE
IN
MECHANICAL ENGINEERING

Bogazici University Library



39001100316051

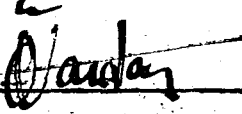
14

Bogazici University

February, 1983

THIS THESIS HAS BEEN APPROVED BY:

Doç.Dr.Öktem VARDAR
(Thesis Supervisor)

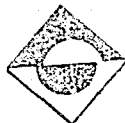
: 

Doç.Dr.M.Başar CİVELEK

: M. Başar Civelek

Dr.Sabri ALTINTAŞ

: S. Altıntaş



ACKNOWLEDGEMENTS

I would like to express my thanks to my thesis advisor Doç. Dr. ÖKTEM VARDAR for his great support throughout this study and to production director of Eskisehir Supply and Maintenance Center Eng. Col. Fazıl AYDINAKINA for machining the specimen.

ABSTRACT

In this thesis "Fatigue-crack initiation in 2024-T3 aluminium alloy" was investigated using experimental methods with compact tension specimens having various notch root radius. The root radii are varied from 0.04 to 2.5 mm.

The fatigue-crack initiation tests were conducted on a closed-loop servo-controlled fatigue testing machine. The loading was tension to tension and frequencies of fatigue tests were 3 Hz. Initiation of fatigue-crack was detected by means of a microscope.

The effects of notch root radius on the fatigue-crack initiation was evaluated by using linear-elastic-fracture-mechanics theory. The results of experiments are plotted, discussed and compared with the results of the previous studies.

ÖZET

Bu tez çalışmasında, 0.04 mm. den 2.5 mm. ye kadar değişen çentik radiuslarına sahip (CTS) deney numuneleri ile deneysel yöntemler kullanarak 2024-T3 alüminyum alaşımı malzemede yorulma çatlaklarının oluşması incelendi.

Yorulma çatlaklarının oluşum deneyleri kapalı devre servo-kontrollü yorulma deney makinasında, çekme-çekme yükleme şartlarında, 3 Hz. yorulma test frekansında yapıldı. Yorulma çatlaklarının oluşması bir mikroskop vasıtasıyla gözlemlendi.

Lineer-elastik-kırılma-mekanik teorisi kullanılarak çentik dibi radiusların, yorulma çatlaklarının oluşması üzerindeki etkileri incelendi.

Deney sonuçları grafik halinde gösterilerek bu konu üzerindeki daha önceki çalışmalarla karşılaştırılarak mukayese edildi.

TABLE OF CONTENTS

LIST OF FIGURES	iv
LIST OF TABLES	v
LIST OF SYMBOLS	vi
I- INTRODUCTION	1
1.1- Fatigue-crack propagation	2
1.2- Fatigue fracture	5
II- APPLICATION OF LINEAR ELASTIC FRACTURE MECHANICS (LEEM) TO FATIGUE-CRACK INITIATION	7
2.1- The elastic-stress field in the vicinity of a crack tip	7
2.2- The elastic-stress field in the vicinity of sharp elliptical or hyperbolic notches	8
2.3- Effect of stress-concentration on fatigue crack initiation	11
III- PREVIOUS WORK	13
IV- EXPERIMENTAL WORK	31
4.1- Material properties	31
4.2- The specimen preparation	33
4.3- Experimental procedure for fatigue-crack initiation	34
4.4- Result and discussion of fatigue crack initia- tion test	37
V- CONCLUSION	43

LIST OF FIGURES

Figure-1.1	Fatigue crack growth rate vs ΔK_I	3
Figure-1.2	K_c v.s B	6
Figure-2.1	The elastic stress field distribution near the tip of the fatigue notch	7
Figure-2.2	The elastic stress field in the vicinity of sharp elliptical or hyperbolic notches	9
Figure-4.1	Compact Tension specimen (CTS)	33
Figure-4.2	Crack detection	35
Figure-4.3	Experimental set-up	36
Figure-5.1	$\Delta\sigma_{nom}$ v.s Ni graph	46
Figure-5.2	$\Delta K_I / \sqrt{\rho}$ v.s Ni graph	47
Figure-5.3	$\Delta K_I / EV\sqrt{\rho}$ v.s Ni graph	48
Figure-5.4	$K_f^N \times \Delta\sigma_{nom}$ v.s Ni graph	49

LIST OF TABLES

Table-1 Fatigue-crack initiation data

Table-2 $\Delta K_1 / \sqrt{\rho} E$ and Ni data

LIST OF SYMBOLS

A	Material constant
a	Crack length
a/W	Crack length-the width of specimen ratio
B	Thickness of specimen
C	Material constant
da/dN	Crack growth rate
E	Young's modulus
K_f^N	Fatigue notch factor by Neuber
K_f^P	Elasto-plastic fatigue notch factor
K_I	Stress intensity factor for mode-I
K_{Ic}	Fracture toughness for mode-I
K_T	Elastic stress concentration factor
ΔK_{th}	Stress intensity range threshold at which the crack growth rate is apparently zero.
ΔK_I	Stress intensity factor range for mode-I
N_i	Number of cycles for fatigue-crack initiation
P	Applied load
ΔP	Applied load fluctuation
$\Delta \sigma_{nom}$	Nominal stress fluctuation
$\Delta \sigma_{max}$	Maximum stress fluctuation
ρ	Notch root radius

CHAPTER - I

INTRODUCTION

The field of fracture mechanics has become the primary approach for controlling brittle fracture and fatigue failures in structures. Brittle fracture of large structures caused large damages in the past.

In 1950's two Commet aircrafts failed catastrophically while at high altitudes. An exhaustive investigation indicated that the failures initiated from very small fatigue-cracks originating from rivet holes near openings in the fuselage.

Numerous other failures of aircraft landing gear and rocket motor cases have occurred from undetected defects or from sub-critical crack growth by fatigue. The failure of F - 111 aircrafts were attributed to brittle fractures of members with preexisting flaws.

Metal fatigue was encountered as a general problem when engineers were faced with difficulties such as failure of railway carriage axles or partial failure of aircraft parts under repeated loads.

It should be considered how fracture mechanics can be used to prevent brittle fracture and fatigue failures of engineering structures.

The fatigue life of structural components is determined by the sum of the elapsed cycles required to initiate a fatigue-crack and to propagate the crack from subcritical dimensions. Consequently, the fatigue life of structural component may be considered to be composed of three continuous stages.

- 1- Fatigue-crack initiation
- 2- Fatigue-crack propagation
- 3- Fatigue fracture

Many studies of fatigue-crack initiation stage at the notch root have proved the great importance of this stage in predicting the fatigue life of structures. They are either for completely elastic [1,2,4] or simplified elasto-plastic analysis [5,6] . Many investigators have studied the other stages [1,7]

1.1- FATIGUE-CRACK PROPAGATION

The fatigue-crack propagation behavior under constant amplitude load fluctuations for metals can be divided into three regions which can be observed in figure-1.1

Region-I exhibits a "Fatigue-threshold" cyclic stress intensity factor fluctuation, ΔK_{th} , below which cracks do not propagate under cyclic-stress fluctuations.

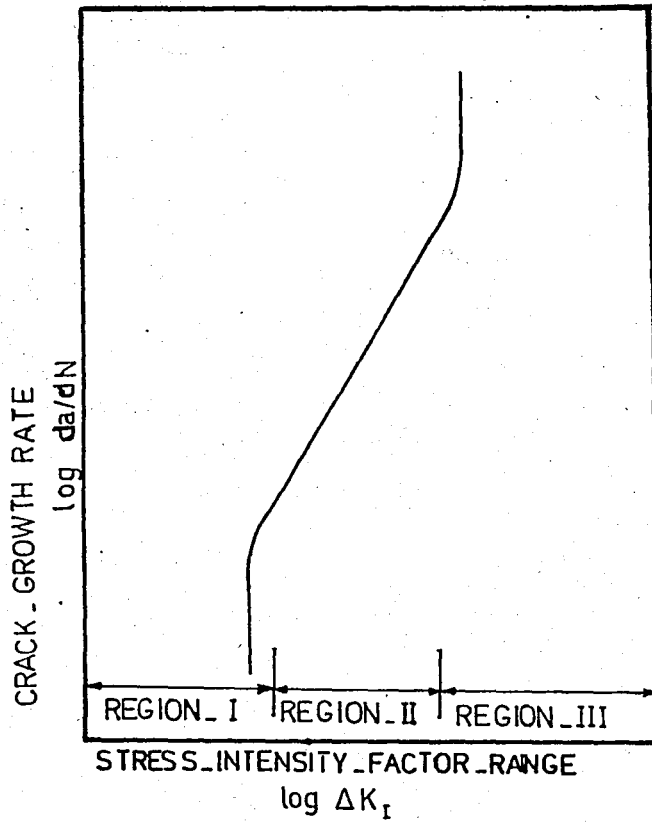


Figure-1.1

Region-II, represents the fatigue-crack propagation behavior above ΔK_{th} , which can be represented by

$$\frac{da}{dN} = c (\Delta K)^m \quad (1.1)$$

Where, $\frac{da}{dN}$ = Fatigue-crack growth rate.

(c) and (m) are constants.

N : Number of cycles.

ΔK : Stress-intensity factor fluctuation,

ΔK can be calculated by,

$$\Delta K = f(g) \sigma \sqrt{a} \quad (1.2)$$

$f(g)$ is a parameter that depends on the specimen and crack geometry.

Number of cycle for fatigue-crack propagation can be predicted by,

$$\int_{N_i}^N dN = \int_{a_0}^a \frac{da}{C(\Delta K)^m} \quad (1.3)$$

In region-III, the fatigue-crack growth per cycle is higher than predicted for region-II. The rate of fatigue-crack growth increases. This increase occurs at a constant value of crack-tip displacement, δ_T , and at a corresponding stress-intensity factor value, K_T , given by,

$$\delta_T = \frac{K_T}{E \sigma_{ys}} \quad (1.4)$$

K_T : Stress-concentration factor value corresponding to onset of acceleration in fatigue-crack growth rates.

E : Young's modulus

σ_{ys} : Yield strength

Acceleration of fatigue-crack-growth rates that determines the transition from region-II to region-III appears to be caused by the superposition of a ductile-tear mechanism. Ductile tear occurs when the strain at the tip of the crack reaches a critical value. Thus, the fatigue-rate transition from region-II to region-III depends on K_{max} and stress ratio, R .

Equation-1.4 is used to calculate the stress-intensity factor value corresponding to the onset of fatigue-rate transition, K_T (or ΔK_T) which also corresponds to the point of transition from region-II to region-III in materials that have high fracture toughness. Acceleration of the rate of fatigue-crack growth occurs at a stress-intensity-factor value slightly below the critical-stress-intensity factor, K_{Ic} .

1.2- FATIGUE FRACTURE

Fatigue fracture occurs when the stress-intensity factor, K , reaches to a critical value, K_c , with increasing the fatigue crack length. Critical-stress-intensity factor, K_c , also depends on the specimen thickness.

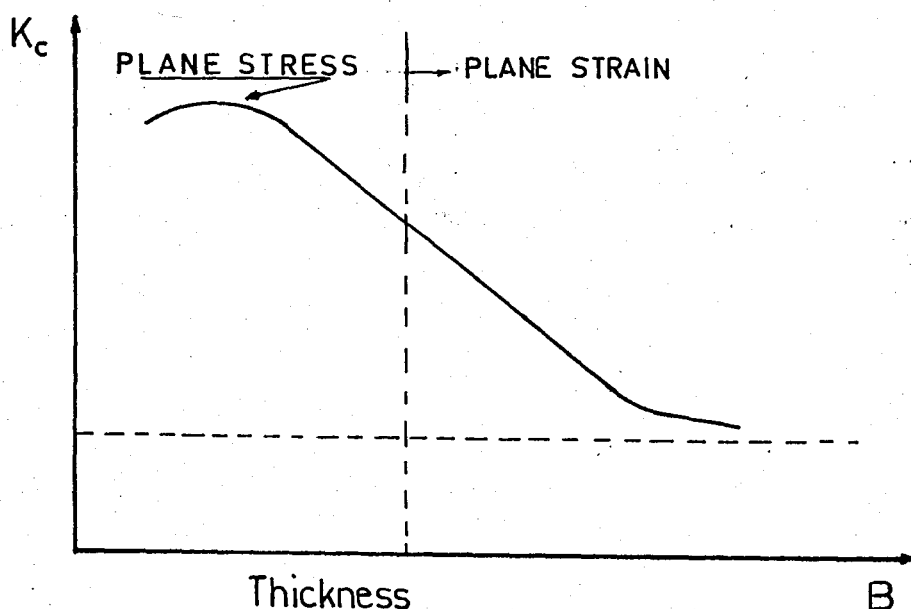


Figure-1.2

The critical-stress-intensity factor, K_c , for a particular structural material, decreases with increasing specimen thickness. In figure-1.2 which shows that the minimum toughness of particular material, K_{Ic} , is reached when the thickness of the specimen is large enough so that the state of stress is plane strain. As the thickness of the specimen is decreased, even though the metallurgical characteristic of the material are not changed, the stress-intensity factor increases and plane-stress, K_c , behavior exits.

CHAPTER - II

APPLICATION OF LINEAR ELASTIC FRACTURE MECHANICS (L.E.F.M)
TO FATIGUE - CRACK INITIATION

Linear-elastic-fracture-mechanics technology is based on an analytical procedure that relates the stress-field magnitude and distribution in the vicinity of a crack-tip to the nominal stress applied to the structure, to size, shape and orientation of a crack and to the material properties.

2.1- THE ELASTIC-STRESS FIELD IN THE VICINITY OF A CRACK-TIP

Figure-2.1 represents σ_x and σ_y components of the elastic-stress field in the vicinity of a crack-tip in a body subjected to tensile stresses normal to the plane of the crack.

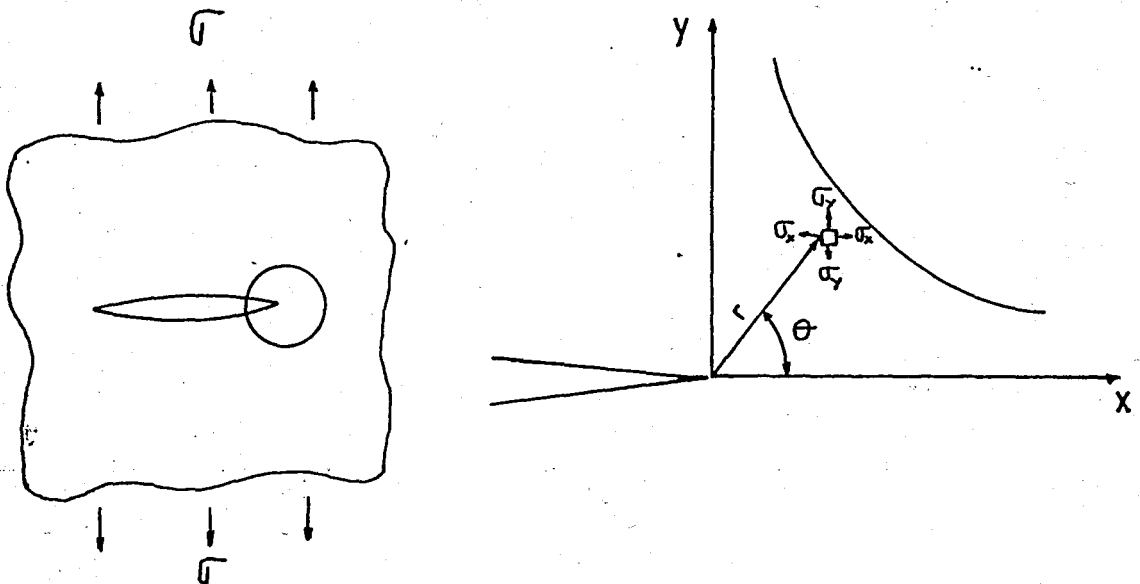


Figure-2.1

The elastic-stress field in the vicinity of a sharp crack is presented by following equations. For MODE-I deformation, in plane-strain,

$$\begin{aligned}\bar{\sigma}_x &= \frac{K_I}{\sqrt{2\pi r}} \cos \frac{\theta}{2} \left[1 - \sin \frac{\theta}{2} \sin \frac{3\theta}{2} \right] \\ \bar{\sigma}_y &= \frac{K_I}{\sqrt{2\pi r}} \cos \frac{\theta}{2} \left[1 + \sin \frac{\theta}{2} \sin \frac{3\theta}{2} \right] \\ \tau_{xy} &= \frac{K_I}{\sqrt{2\pi r}} \sin \frac{\theta}{2} \cos \frac{\theta}{2} \cos \frac{3\theta}{2}\end{aligned}\tag{2.1}$$

$$\bar{\sigma}_z = \nu (\bar{\sigma}_x + \bar{\sigma}_y) \quad \tau_{xz} = \tau_{yz} = 0$$

$$u = \frac{K_I}{G} \left[\frac{r}{2\pi} \right]^{1/2} \cos \frac{\theta}{2} \left[1 - 2\nu + \sin^2 \frac{\theta}{2} \right]$$

$$v = \frac{K_I}{G} \left[\frac{r}{2\pi} \right]^{1/2} \sin \frac{\theta}{2} \left[2 - 2\nu - \cos^2 \frac{\theta}{2} \right]$$

$$w = 0$$

Where, the stress components and the coordinates (r) and (θ) are presented in figure-2.1. K_I is the stress-intensity factor by the help of which the magnitude of the elastic-stress field can be described.

2.2- THE ELASTIC-STRESS FIELD IN THE VICINITY OF SHARP ELLIPTICAL OR HYPERBOLIC NOTCHES

The elastic-stress field in the vicinity of sharp elliptical or hyperbolic notches in a body subjected to tensile stresses

normal to the plane of notch is presented by the following equation.

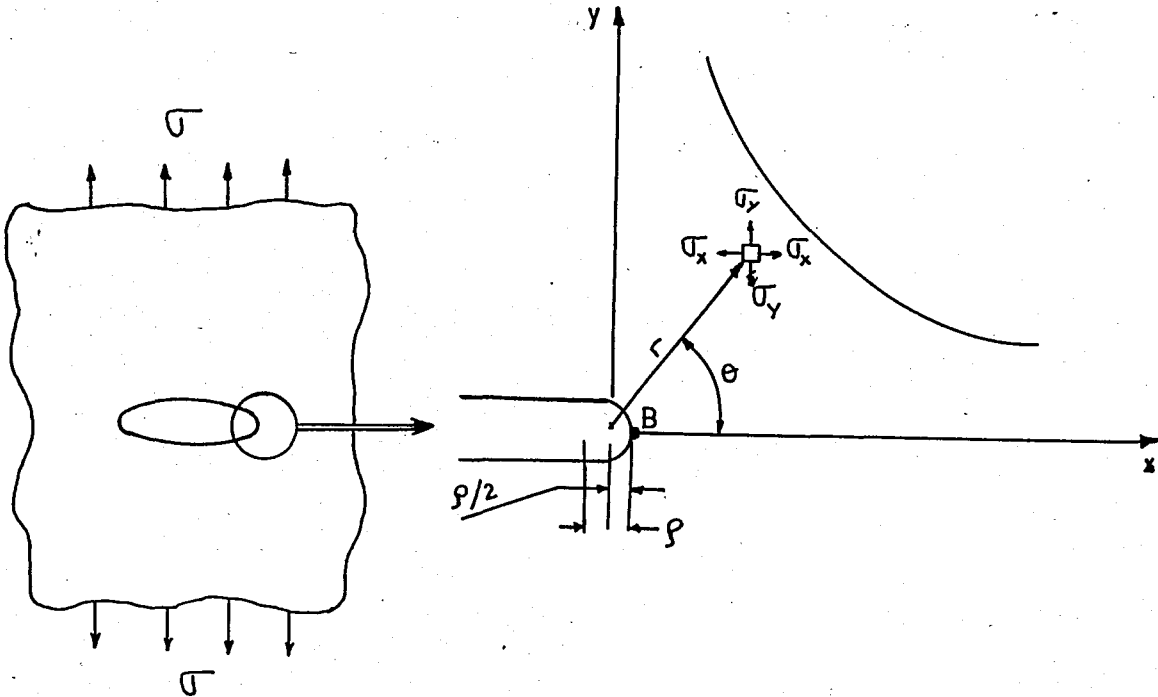


Figure-2.2

$$\sigma_x = \frac{K_1}{\sqrt{2\pi r}} \cos \frac{\theta}{2} \left[1 - \sin \frac{\theta}{2} \sin \frac{3\theta}{2} \right] - \frac{K_1}{\sqrt{2\pi r}} \frac{\rho}{2r} \cos \frac{3\theta}{2}$$

$$\sigma_y = \frac{K_1}{\sqrt{2\pi r}} \cos \frac{\theta}{2} \left[1 + \sin \frac{\theta}{2} \sin \frac{3\theta}{2} \right] + \frac{K_1}{\sqrt{2\pi r}} \frac{\rho}{2r} \cos \frac{3\theta}{2}$$

$$\tau_{xy} = \frac{K_1}{\sqrt{2\pi r}} \sin \frac{\theta}{2} \cos \frac{\theta}{2} \cos \frac{3\theta}{2} - \frac{K_1}{\sqrt{2\pi r}} \frac{\rho}{2r} \sin \frac{3\theta}{2}$$

(2.2)

Where, the coordinates (r) and (θ) , (ρ) are defined in figure-2.2

The first term in equation-2.2 defines the magnitude and distribution of the stress-field in the vicinity of a sharp crack. In this equation, K_I , is the stress-intensity factor. The second term in this equations represents influence of a blunt-tip radius on this stress field.

At point (B), in figure-2.2, for $\theta=0$; $r=\rho/2$

Equation-2.2 becomes,

$$\begin{Bmatrix} \sigma_x \\ \sigma_y \\ \tau_{xy} \end{Bmatrix} = \frac{K_I}{\sqrt{\pi\rho}} \begin{Bmatrix} 0 \\ 2 \\ 0 \end{Bmatrix} \quad (2.3)$$

and the material element at the tip of the notch in cyclically loaded structural component is subjected to the maximum stress σ_{max} , and to the maximum stress fluctuations, $\Delta\sigma_{max}$, consequently, this material element is most susceptible to fatigue damage and is, in general, the origin of fatigue-crack initiation. For $r=\rho/2$ the maximum stress fluctuation on this material element which can be derived from equation-2.3 is,

$$\Delta\sigma_{max} = \frac{2 \Delta K_I}{\sqrt{\pi\rho}} \quad (2.4)$$

Where, ΔK , is the stress-intensity factor fluctuation. Although equation-2.4 is considered exact only when (ρ) approaches zero. Wilson and Gabrielse [8] showed by using finite element analysis of blunt notches in compact tension specimens that this relationship is accurate to within 10 % for notch root radii up to 0.180 in.

2.3- EFFECT OF STRESS CONCENTRATION ON FATIGUE-CRACK INITIATION

The effect of geometrical discontinuity in a loaded structural component is to intensify the magnitude of the nominal stress in the vicinity of the discontinuity. The localized stresses may cause the metal in that neighborhood to undergo plastic deformation. Because the nominal stresses in most structures are elastic the zone of plastically deformed metal in the vicinity of stress concentrations is surrounded by an elastic stress field. To predict the effect of stress concentrations on the fatigue behavior of structures, the fatigue behavior of the localized plastic zones has been simulated by testing smooth specimens under strain-controlled conditions.

A better simulation of the effects of stress concentrations on the fatigue behavior of structures is obtained by testing notched specimens under stress-controlled conditions because the applied stress can be more directly related to the struc-

tural loading. The number of load fluctuations required to initiate a fatigue-crack in the vicinity of a notch tip is related to $\Delta K_1 / \sqrt{\rho}$, which in turn is related to the maximum alternating stress in the vicinity of the notch tip.

In the linear-elastic-fracture-mechanics theory, fatigue-cracks do not initiate in structural components when the body configuration, the notch geometry and nominal stress fluctuations are such that the magnitude of the parameter $\Delta K_1 / \sqrt{\rho}$, is less than a given value, which is called threshold value. In general, the value of this fatigue-crack initiation threshold, $(\Delta K_1 / \sqrt{\rho})_{th}$, increases with increasing yield strength or tensile strength of the material.

W

CHAPTER-III

PREVIOUS WORK

PEARSON (1) investigated the effect of notch depth and root radius on fatigue-crack initiation and propagation in half inch thick specimens aluminium alloys.

He used three-point bending specimens. The test specimen dimensions were 1 in. x 1/2 in. extruded bar B.S specification L 65. The specimen were fatigued in bending machine. Loading was tension to tension. The cyclic load speed was 1500 cycles per minute and subsequent crack propagation is measured using the electrical resistance method.

He expressed that, for the same value of $\Delta K_I / \sqrt{\rho}$ the notches with low values of K_T have short initiation times. While the law,

$$N_i = C \left[\frac{\Delta K_I}{\sqrt{\rho}} \right]^{-5} \quad (3.1)$$

give a rough approximation, it does not exactly represent the results. In $\log N_i$ v.s $\log (\Delta K_I / \sqrt{\rho})$ graph for a single notch depth and root radius, the test results lie on a straight line of slope 5. When $\log N_i$ versus $\log (\Delta K_I / \sqrt{\rho})$ is plotted, it is seen that for

the same root radius and a single notch depth, the overall scatter is greater than obtained Jack and Price [2].

The other approach was related to the fatigue stress concentration factor (K_f) which was defined

$$K_f = \frac{\text{Stress to produce failure in a given number of cycles in unnotched test pieces.}}{\text{Net section stress to produce failure in same number of cycles in notched test pieces.}}$$

For fatigue-crack initiation, K_{fi} was defined as the ratio of the stress producing failure in unnotched test pieces in a given number of cycles to the stress initiating the crack in the same number of cycles in notched pieces.

The test results showed that the value of K_T/K_{fi} was almost constant for $\rho \geq 0.01$ in. and equal to 1.35 so that crack initiation can be represented by the equation,

For L 65 aluminium alloy;

for $\rho \geq 0.01$ in.

$$\sigma_{NSi} = \frac{1.35}{K_T} \sigma_f \quad (3.2)$$

Where; $\bar{\sigma}_{NSi}$ = Net section stress to initiate a crack
0.005 in. long in N cycles.

$\bar{\sigma}_f$ = Failure stress for unnotched test pieces
in N cycles.

It should be noted that there is a size effect in fatigue results for notched specimens.

A.R.JACK and A.T.PRICE [2] investigated the initiation of fatigue-cracks from notches in mild steel plates. They used single-edge notched specimens of mild steel in their experimental work.

Test were carried out at room temperature on a testing machine of 10 000 lb. capacity. All tests were carried out at 20 cpm under zero to tension or tension to tension conditions.

The major variables investigated were notch depth (a) and root radius (ρ). Three types of specimens were tested in experimental work and they had different width (w) and thickness (B). Tests were carried out at stress amplitudes in the range 1000 lbf/in² to 3500 lbf/in² measured on the gross section, under conditions producing failure in less than about 2×10^5 cycles. Crack initiation was detected by using electrical potential drop of about 1mV over 1 in. of uncracked specimens.

They showed that number of cycles to initiate a fatigue-crack was proportional to the range of stress-intensity factor

(ΔK) for sharp notches which have $\rho \leq 0.010$ in. the test data was analysed by plotting N_i against the stress-intensity factor range. It was noted that the slope of this line was (4) and N_i was proportional to $(\Delta K)^{-4}$

i.e.

$$N_i \propto (\Delta K)^{-4} \quad (3.3)$$

within the ranges studied, there was no effect of width or thickness.

Test on specimens having notch root radius greater than 0.010 in. showed that N_i increasing with increasing root radius. At particular values of (a) and (\sqrt{r}), the relationship indicated was

$$N_i \propto \sqrt{\rho} \quad (3.4)$$

If the relationship is analysed clearly, for the notch root radius values which are greater than critical notch root radius (0.010 in.), it can be noted that the number of cycle to initiate a fatigue-crack is a function of $\Delta K/\sqrt{\rho}$.

Y.H.KIM, T.MURA and M.E.FINE [3] investigated fatigue-crack initiation and microcrack growth in 4140 steel in three conditions, as-quenched, tempered at 400°C and tempered at 600°C.

Specimens 90x20x3.2 mm size were machined from 3.5 mm thick plates. The specimens were austenitized in Argon for one hour at 1000°C and then oil-quenched and with two different tempering conditions were investigated, one hour at 400°C or 650°C in vacuum.

Single-edge notched specimens were used in the experimental study. The specimens have a crack 1 mm long (a) and with 0.22 mm radius of curvature (ρ). Only one notch geometry was investigated.

All fatigue tests were conducted on a closed-loop electro-hydraulic MTS machine of 90 KN capacity at room temperature using 30 Hz. test frequency. Fatigue-crack initiation was detected by a metallurgical microscope.

They indicated the results for crack initiation in the 4140 steel samples for each of three conditions in the graphs. They defined N_{ii} as the number of cycles to initiation 3 μm crack and N_{if} as the number of cycles to form a crack extending across the full lateral dimensions of the notch i.e 3.2 mm.

For as-quenched 4140 steel, very few cracks formed near the notch edges. Furthermore, once the crack initiated, it grew rapidly to the fatal crack and N_{if} was not much greater than N_{ii} .

For 650°C tempered samples approximately 100 fatigue-cracks formed near the edges of notch and these grew very slowly or not at all.

For 400 and 650°C tempered specimens N_{if} was considerably larger than N_{ii} . They suggested that the N_{ii}/N_{if} ratio could be approximately 0.1 and microcracks grew most rapidly in as-quenched specimens and least rapidly in 650°C tempered specimens at the same $\Delta K / \sqrt{\rho}$.

In as-quenched specimens, fatigue-cracks initiated at grain boundaries but in the 400 and 650°C tempered specimens, they initiated at intrusions-extrusions.

The experimental results for the threshold values of $\Delta K / \sqrt{\rho}$ were compared to the $\Delta K / \sqrt{\rho} |_{th} = 26 \times (\sigma_{ys})^{1/2}$ which was BARSOM's new correlation. The agreement with the new BARSOM formula was much better than with the old formula which was $\Delta K / \sqrt{\rho} |_{th} = 9.5 \times (\sigma_{ys})$.

The experimental results are plotted in $\log[\Delta K / \sqrt{\rho} - \Delta K / \sqrt{\rho} |_{th}]$ v. $\log N_{if}$ graph. The data fit reasonably well to straight line.

They suggested that the crack initiation data for 4140 steel were fit to the empirical equation.

$$N_{if} = (\Delta K / \sqrt{\rho} - \Delta K \sqrt{\rho} |_{th}) \quad (3.5)$$

J.M.BARSON and R.C.McNICOL [4] investigated effect of stress concentration on fatigue-crack initiation in HY-130 steel.

They used double-edge-notched specimens which were 20 in. long, 6 in. wide, and 0.125 in. thick. Notch tip radii were changed from 0.008 in. to 0.375 in. The polished, unnotched specimens, that were tested, had 10 in. radius.

All specimens were tested at room temperature in 50 kip on MTS. The frequency of stress fluctuation was 120 to 600 cpm. Fatigue-crack initiation was detected optically with a stereo-zoom microscope. The specimens were tested over a range of fluctuating stress and number of cycles required to initiate a 0.01 in. crack was recorded. The variation of notch acuity covered the range from fatigue-cracked specimens to polished, unnotched specimens and fatigue-crack initiation data were obtained in the range 10^3 to 10^6 cycles. The data were analyzed by using linear-elastic-fracture-mechanics concepts and theory of stress concentration in notched specimens.

Their results showed that the number of elapsed load cycles required to initiate a fatigue-crack in notched specimens is related to the ratio of the fluctuation of stress intensity factor ΔK_I to the square root of the notch tip radius (ρ). Fatigue-crack initiation life can also be expressed in terms of the fluctuation of the maximum stress at the notch tip ($\Delta \sigma_{max}$) because $\Delta K_I / \sqrt{\rho}$ can be related to ($\Delta \sigma_{max}$).

Fatigue-crack initiation threshold was investigated in HY-130 steel by BARSOM and McNICOL. The data indicated that fatigue-cracks did not initiate in steel structural components when the body configuration, the notch geometry and nominal-stress fluctuations were such that the magnitude of the parameter $\Delta K_I/\sqrt{\rho}$ was less than a given characteristic value of steel. In general, the value of this fatigue-crack initiation threshold $(\Delta K_I/\sqrt{\rho})_{th}$ increased with increasing yield strength or tensile strength of the steel.

They showed that fatigue-crack initiation threshold at $\Delta K_I/\sqrt{\rho} = 85 \text{ Ksi}$ was reasonably applicable to notches having a stress-concentration factor value, K_t , that ranged from 17.2 for the specimen with $\rho=0.008 \text{ in.}$ to 2.9 in. for the specimens with $\rho=0.375 \text{ in.}$

They suggested that the fatigue-crack initiation threshold in martensitic steels of various yield strengths tested under zero to tension load fluctuation can be predicted by the equation.

$$\frac{\Delta K_I}{\sigma_{ys} \sqrt{\rho}} = 0.6 \quad (3.6)$$

The use of this relationship to predict the fatigue-crack initiation threshold in various metal alloys may require normalizing the relationship with respect to Young's modulus, E , or some power of E .

The test data showed that, in the finite-initiation life region, the number of elapsed cycles required to initiate a fatigue crack at the tip of a notch, N_i , is related to the parameter $\Delta K_I / \sqrt{\rho}$ by the equation

$$N_i = \beta \frac{1}{(\Delta K_I / \sqrt{\rho})^n} \quad (3.7)$$

Where, β is a constant and the value of exponent, (n) , decreases.

The data also showed that at a constant value of the parameter, $(\Delta K_I / \sqrt{\rho})$, the number of cycles required to initiate a fatigue-crack in the region of finite cyclic life, increased as the notch-tip radius increased.

A. BAUS, H. P. LIEURADE, G. SANZ, and M. TURCHON [5] investigated fatigue-crack initiation at the root of a notch. The specimen material was two kinds of high-strength steels (AFNOR 35 NCD 16 and 35 NCD 4). They used compact tension specimen, 15 mm thick,

having various notch root radii between 0.003 in. and 0.04 in. All crack initiation testing was conducted on a servo-hydraulic fatigue machine of ± 100 KN under tension to tension loading conditions and at a frequency of 20 Hz. In order to detect fatigue-crack initiation in the center of the specimen, they used two methods which were compliance measurement and potential drop method.

They showed that for the same notch root radius, the test points lie on a straight line. If the number of cycles to initiate a fatigue-crack is to be kept constant a higher load amplitude must be applied to the specimen for increasing the stress intensity fluctuating as the notch root radius increases. When the N_1 v.s $\Delta K_1/\sqrt{\rho}$ diagram was plotted, it was noted that the points still lie on straight lines at constant notch root radius, but corresponding $\Delta K_1/\sqrt{\rho}$ levels decreases as the root radius (ρ) increases.

Another approach of elastic analysis is fatigue notch factor (K_f) which is characteristic of both the mechanical notch and material. K_f is defined as the ratio of the fatigue limits of unnotched specimens and a notched specimen, during tests of the same type.

It was not possible to carry out a comparison with tests on unnotched specimens when the notched ones were compact. Thus they used Neuber's empirical formula to define the notch factor which was,

$$K_f^N = 1 + \frac{K_T - 1}{1 + \sqrt{A/\rho}} \quad (3.8)$$

Where, K_T , is the stress concentration factor and A is a material constant.

Knowing K_f^N , it was possible to calculate the amplitude of the maximum stress at the notch root by the formula,

$$\Delta \sigma_{\max}^N = K_f^N \times \Delta \sigma_{\text{nom}} \quad (3.9)$$

In elasto-plastic analysis of stress concentration, the modified Neuber rule was a powerful means of expressing notch root stress-strain behavior.

$$K_f^2 = K_\sigma \times K_\epsilon \quad (3.10)$$

$$K_\sigma = \frac{\Delta \sigma}{\Delta \sigma_{\text{nom}}} \quad (3.11)$$

$$K_\epsilon = \frac{\Delta \epsilon}{\Delta \epsilon_{\text{nom}}} \quad (3.12)$$

and ;

$$K_f \times \Delta \sigma_{\text{nom}} = \sqrt{E \cdot \Delta \sigma \cdot \Delta \epsilon} \quad (3.13)$$

After each initiation test, it is verified that for a given material and given value of K_T the ratio $\sqrt{E \cdot \Delta \sigma \cdot \Delta \epsilon} / \Delta \epsilon_{nom}$ remained constant whatever the value of N_i with only a small scatter in the values around an average value which they call K_f^{EP} . Knowing the values of K_f^{EP} for each material and each notch configuration, they presented the test results relating $K_f^{EP} \times \Delta \sigma_{nom}$ and N_i in a graph.

K_f^N , the fatigue notch factor and K_f^{EP} , elasto-plastic initiation parameter which can be calculated from the Manson-Coffin curve and cyclic stress-strain curve of the material. They suggested that these parameters did not yield the same accuracy for the calculation of the number of cycles N_i . The K_f^{EP} approach showed that there exists a good correlation between fatigue-crack initiation when $N_i < 10^5$ cycles and materials low-cycle fatigue behavior.

They were in good agreement with BARSOM who suggested that the elastic $(\Delta K / \sqrt{\rho})_{th}$ approach was very helpful when $N_i > 10^6$ cycles. $(\Delta K / \sqrt{\rho})_{th}$ defines a threshold value under which no crack occurs.

K.SAANOUNI and C.BATHIAS [6] studied on the fatigue-crack initiation in the vicinity of notches of the 316 austenitic stainless steel. They used 28 notched compact tension specimens with two different widths, various notch depth (a) and root radii (ρ).

Crack-initiation testings were conducted on hydraulic fatigue test machine. The loading condition was tension to tension and frequencies vary between 0.1 and 5 cps. in air environment and room temperature. Fatigue-crack initiation was detected by three different monitoring techniques.

One procedure involved electrical potential variation with time. The second procedure involves crack opening displacement variation versus time and third one, the use of scaled microscope mounted at both polished sides of compact tension specimens.

Their test results showed that for the same N_i , $\Delta\sigma_{nom}$ increased when notch root radius increased. The real stress amplitude at the notch tip $\Delta\sigma_{max}$ was

$$\Delta\sigma_{max} = K_T \Delta\sigma_{nom} = \frac{2}{\sqrt{\pi}} \frac{\Delta K}{\sqrt{\rho}} \quad (3.14)$$

For both parameters ($\Delta K/\sqrt{\rho}$ and $K_T \Delta\sigma_{nom}$) it is assumed that initiation was an elastic phenomenon neglecting the plasticity deformation at tip of the notch. They defined a critical value for notch root radius (ρ_c) below which the number of cycles N_i was independent of $\frac{\sigma_{min}}{\sigma_{max}}$. The critical notch root radius was found to be 0.25 mm.

Although the nominal stress range may be elastic, there is always a plastic zone which caused by the localized stresses at

the notch root. Therefore the elasto-plastic analysis was used to predict the number of cycles to initiate a fatigue-crack.

A function of damage is defined as, $(\sqrt{E \cdot \Delta \sigma \cdot \Delta \epsilon})$

$$K_T^2 = K_\sigma \times K_\epsilon \quad (3.15)$$

$$K_\sigma = \frac{\Delta \sigma_{nom}}{\Delta \sigma} \quad (3.16)$$

$$K_\epsilon = \frac{\Delta \epsilon_{nom}}{\Delta \epsilon} \quad (3.17)$$

K_f is introduced instead of K_T in the above relation and if the nominal stress range $\Delta \sigma_{nom}$ is limited within elastic range and

$$\Delta \epsilon_{nom} = \frac{\Delta \sigma_{nom}}{E} \quad (3.18)$$

thus,

$$K_f \times \Delta \sigma_{nom} = \sqrt{E \cdot \Delta \sigma \cdot \Delta \epsilon} \quad (3.19)$$

where both $\Delta \sigma$ and $\Delta \epsilon$ were calculated using the cyclic stress-strain curve and Manson-Coffin one for each N_i .

The variation of damage function versus N_i showed that all the test results, lie on one unique line for two types of specimens and all notch root radii.

This could be expressed as;

$$N_i = \left[\psi / \sqrt{E \cdot \Delta \sigma \cdot \Delta E} \right]^{1/\alpha} \quad (3.20)$$

Where, (ψ) and (α) are material constants. In equation-3.9 $\Delta \epsilon = \Delta \epsilon_e + \Delta \epsilon_p$ in which the plastic deformation is not neglected. In using $K_f \cdot \Delta \sigma_{nom}$ one must also take into account the plastic deformation. But $\Delta \sigma_{nom}$ is calculated by neglecting this fact. So the only parameter that can take into consideration for plasticity is the fatigue notch factor K_f , called K_f^P .

The Neuber relation,

$$K_f = 1 + \frac{K_f - 1}{1 + \sqrt{A/\rho}} \quad (3.21)$$

Where A is defined by Neuber to be a material constant which represents the distance from notch tip after which there is no more stress gradient.

$$A = \left[(K_r - K_f) / (K_f - 1) \right]^2 \times \rho \quad (3.22)$$

In constant amplitude test with different values of ΔK (or ΔP), for the same notch geometry, they showed that the function (A) depended not only on the material but also on K which generated the plastic zone size.

$$A = \Psi (\text{material}, r_y) \quad (3.23)$$

Monotonic plastic zone is, where the material is monotonically plastically deformed, its size is;

$$r_{ym} = \frac{1}{6\pi} \left[K_{\max} / \sigma_y \right]^2 \quad \text{if} \quad \Delta \sigma_{\text{nom}} \geq \sigma_y \quad (3.24)$$

Cyclic plastic zone is where the material is deformed plastically in a reversible manner, its size is;

$$r_{yc} = \frac{1}{6\pi} \left[\Delta K / 2\sigma_y \right]^2 \quad \text{if} \quad \Delta \sigma_{\text{nom}} < \sigma_y \quad (3.25)$$

To define the function Ψ , they plot the values of A calculated using equation-313 versus (r_y) and they found,

$$A = 0.02 \exp(1.87 \sqrt{r_y}) \quad (3.26)$$

Introducing Neuber relation, they obtained

$$K_f^P = 1 + \left[(K_t^* - 1) / (1 + (0.02 \exp(1.87 \sqrt{r_y})) / \rho)^{1/2} \right] \quad (3.27)$$

Where K_t^* is the theoretical elastic stress concentration factor calculated from the critical notch root radius.

Plotting the relation between $K_f^P \times \Delta \sigma_{nom}$ and N_i , it was suggested that to predict the number of cycles to initiate a fatigue-crack, the below formula could be used

$$N_i = \left[A' / (K_f^P \times \Delta \sigma_{nom}) \right]^{1/\alpha'} \quad (3.28)$$

Where, A' and α' were constant for 316 austenitic stainless steel.

The test results showed that the localized material element in the tip of the notch, is plastically deformed and crack initiation needs to be studied by an elasto-plastic analysis. Although the analysis based on function of damage ($\sqrt{E \cdot \Delta \sigma \cdot \Delta \epsilon}$) gave better results in prediction of N_i . The real values of $\Delta \sigma$ and $\Delta \epsilon$ are obtained by experimental techniques. On the other hand, the analysis based on elasto-plastic fatigue notch

factor K_f^P was more advantageous for simple prediction of N_i .
The function of A' needs to be well defined in the elasto-
plastic analysis.

CHAPTER - IV

EXPERIMENTAL WORK

4.1- MATERIAL PROPERTIES

The material used throughout this experimental study was 2024-T3 type of Aluminium alloy, with the chemical composition and mechanical properties as below [14]

CORE	Fe	Cu	Mn	Mg	Zn	Ti	Va	Zi	Silicon
%	0.5	5.8 - 6.8	0.2 - 0.4	0.02	0.1	0.02 - 0.01	0.05	0.10	0.5

ASTM number : B 209

Government number : QQ - A - 250

Typical uses : Aircraft structures, rivets, hard ware
truck wheels, screw-machine products e.t.c.

Density : at 68°F (20°C) 2.77 kg/cm³ 0.100 lb/in³

Liquidus temp. : 1180°F (638°C)

Solidus temp. : 935°F (502°C)

<u>Thermal expansion</u>	<u>micro-in/in/°C</u>
-76 to +68°F (-60 to +20°C)	21.4
68 to 212°F (20 to 100°C)	22.8
68 to 392°F (20 to 200°C)	23.9
68 to 572°F (20 to 300°C)	24.7

- Specific heat at 212°F (100°C) : 0.23 cal/g.
Thermal conductivity at 77°F : 0.29 cal/cm²/cm/°C/sec.
Electrical conductivity : 30 % IACS
Electrical resistivity at 68°F : 5.75 microhm-cm
Rockwell hardness : 83-87 RH(B)
Brinell hardness : 120 (500 kg load 100 mm ball)
T3 Heat treatment : Solution heat treated and then cold
worked by flattening operation.

Mechanical properties of 2024-T3 Aluminium alloy plate:

- Ultimate tensile strength : $\sigma_{ult} = 64000 \text{ lb/in}^2 = 45 \text{ kg/mm}^2$
Tensile yield strength : $\sigma_{TYS} = 42000 \text{ lb/in}^2 = 29.5 \text{ kg/mm}^2$
Compressive yield strength : $\sigma_{CYS} = 45000 \text{ lb/in}^2 = 31.6 \text{ kg/mm}^2$
Critical stress intensity factor : $K_c = 40000 \text{ lb/in}^{3/2} = 140 \text{ kg/mm}^{3/2}$
Elongation : 18 %
Modulus of elasticity : $10.6 \times 10^6 \text{ lb/in}^2 = 0.75 \times 10^6 \text{ kg/cm}^2$
Fatigue limit : 17-20 kg/mm²

4.2-THE SPECIMEN PREPARATION

The specimen have been prepared in the department of Jet motor of Eskisehir Supply and Maintenance Center before going on with testing on electro-hydraulic closed loop (MTS 812) fatigue testing machine.

Fatigue-crack initiation tests are performed with the compact tension specimen which is single-edge notched and pin loaded in tension. The geometry of the compact tension specimen and notch are shown in figure-4.1

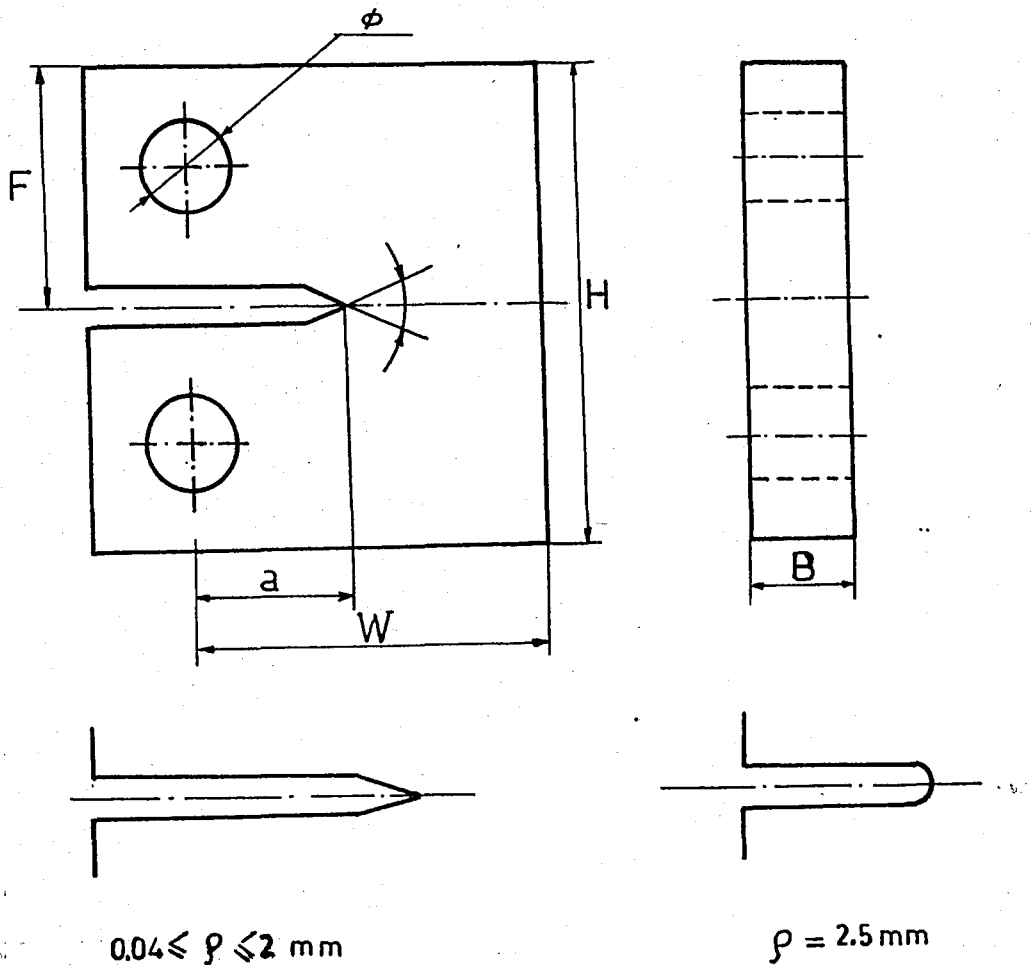


Figure-4.1

In this study, Dimensions are chosen such as;

$$W = 45 \text{ mm}$$

$$a = 21 \text{ mm}$$

$$H = 55 \text{ mm}$$

$$B = 10 \text{ mm}$$

$$F = 22.5 \text{ mm}$$

$$\phi = 10 \text{ mm}$$

The specimen were cut the notch being in the rolling direction of 15 mm thickness Aluminium alloy plate and marked. The pin holes, root radii and notches were machined using a sharp milling cutter. The notch radii vary from 0.04 mm to 2.5 mm; the notches were cleaned and polished by shoot peening.

4.3-EXPERIMENTAL PROCEDURE FOR FATIGUE-CRACK INITIATION

Crack initiation tests were conducted on electro-hydraulic closed loop (MTS 812) fatigue testing machine with a maximum capacity of 10 tons, under sinusoidal tension to tension loading condition at constant amplitudes for all tests.

The test frequencies are 3 Hz. and the conditions are standard with ambient room temperature. Fatigue-crack initiation is detected by means of a Gaertner Travelling Microscope (10X) The microscope is mounted such that one can look directly into

the notch root (figure-4.2) and scan the notch root across the thickness (B) for incipient crack growth.

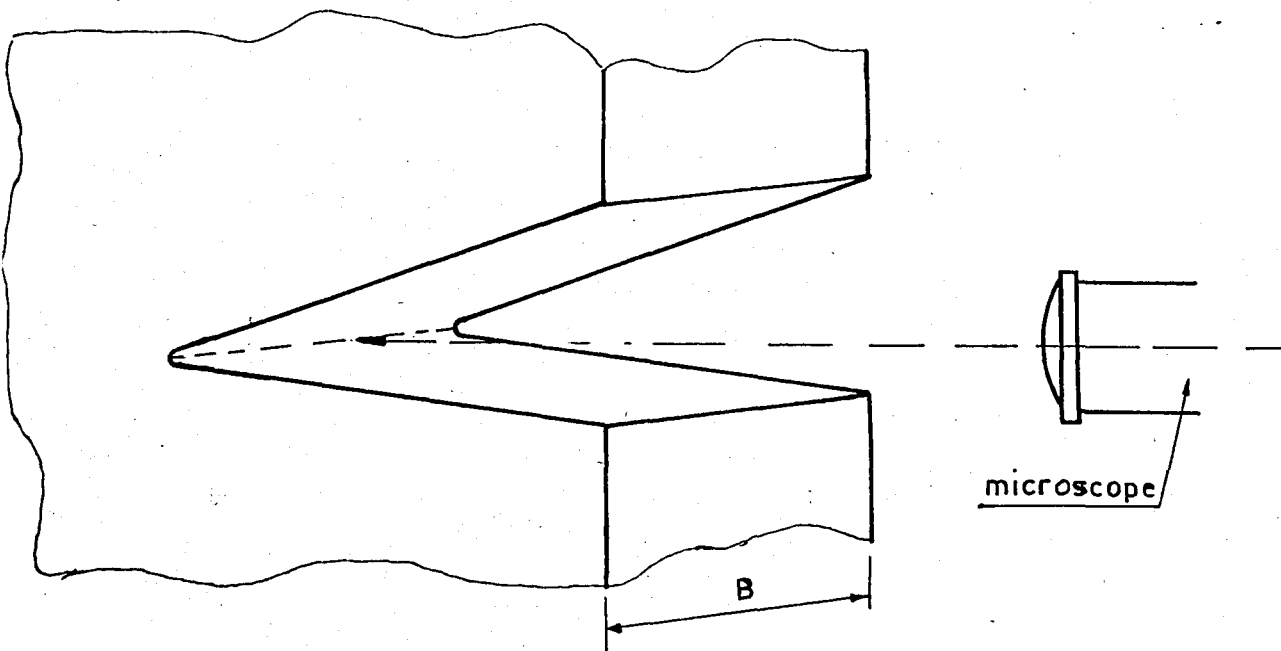


Figure-4.2

Each test is terminated when fatigue-crack initiation is observed at the notch root on the microscope and the number of cycles is recorded. The applied load selected from 40 kg to 650 kg for different specimens having different notch root radius. The applied load monitored through a digital voltmeter. The number of load cycles is counted by the MTS fatigue testing machine.

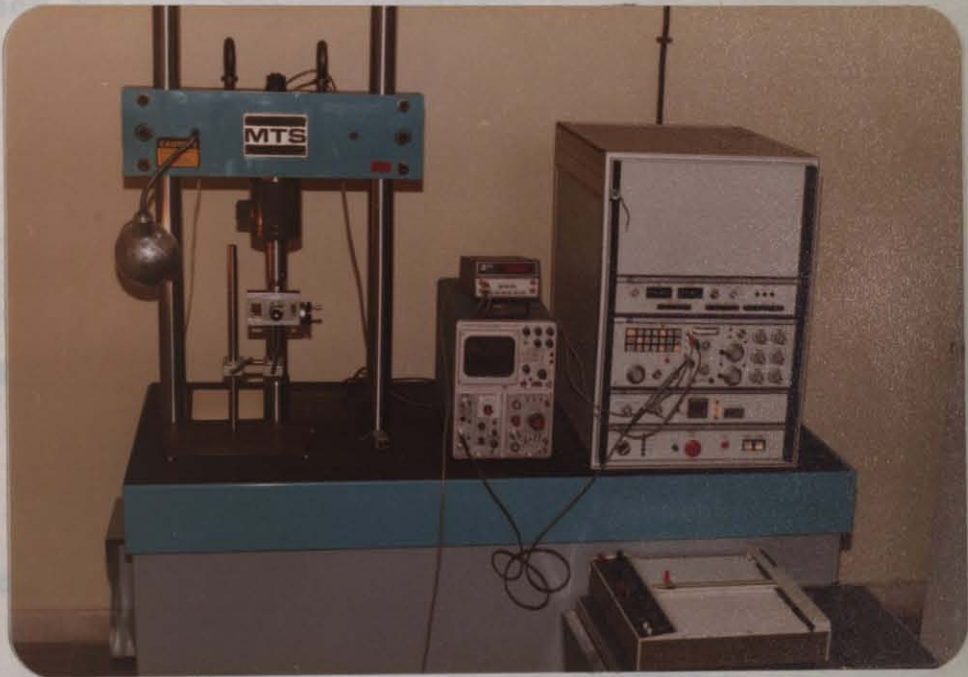


Figure-4.3 EXPERIMENTAL SET-UP

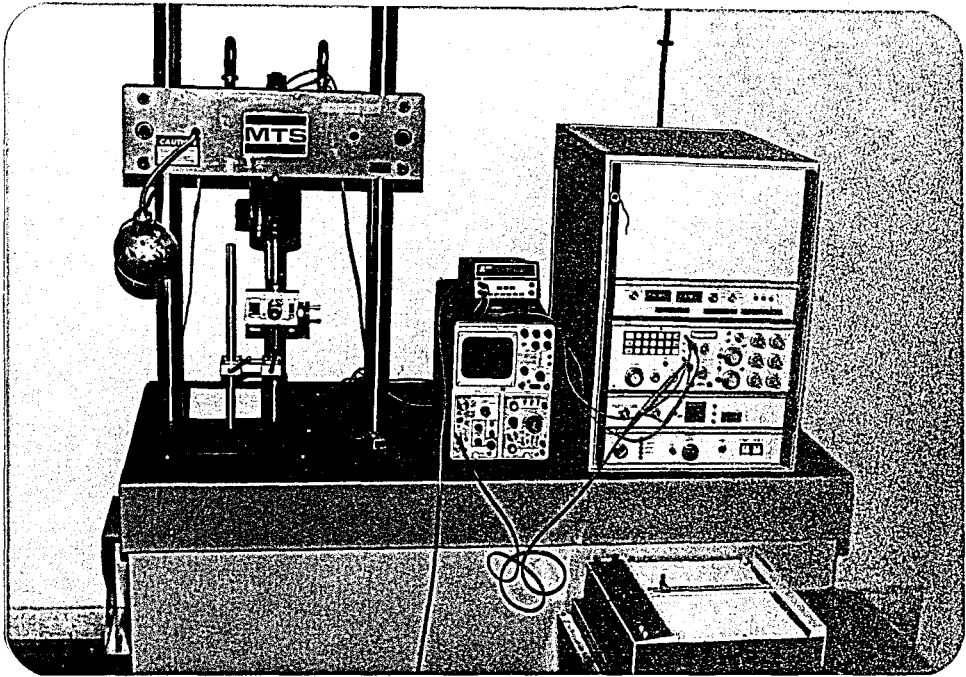


Figure-4.3 EXPERIMENTAL SET-UP

4.4- RESULT AND DISCUSSION OF FATIGUE-CRACK INITIATION TEST

All of the fatigue-crack initiation test results are summarized in table - 1

Maximum alternating stress can be calculated by equation- ΔK_I is the stress-intensity fluctuation which is obtained for compact tension specimen as [8]

$$\Delta K_I = \frac{\Delta P}{B \sqrt{W}} f(a/W) \quad (4.1)$$

$$f(a/W) = 29.6(a/W)^{1/2} - 185.5(a/W)^{3/2} + 655.7(a/W)^{5/2} - 1017(a/W)^{7/2} + 638.9(a/W)^{9/2}$$

Where;

ΔP : Applied load

B : Thickness of the specimen

W : Width of the specimen

a : Crack length

Nominal stress fluctuation is calculated by the equation-
For compact tension specimen [6]

It is given as;

$$\Delta \sigma_{nom} = \frac{\Delta P}{B(W-a)} \left[1 + \frac{3(W+a)}{(W-a)} \right] \quad (4.2)$$

The fatigue-crack initiation behavior of the specimen is presented in figure-5.1, in terms of the number of cycles for fatigue-crack initiation, N_i , versus the nominal stress fluctuation, $\Delta \sigma_{nom}$.

The data presented in figure-5.1 for $\rho=1.5$ mm, show that the number of cycles to initiate a fatigue-crack in the low-cycle region, which is defined $N_i \leq 5 \times 10^4$ cycles, can be calculated by

$$N_i = A (\Delta \sigma_{nom})^{-n} \quad (4.3)$$

Where, for $\rho=1.5$ mm	$n=1.88$	$A=6.5 \times 10^6$
$\rho=0.5$ mm	$n=1.72$	$A=8.1 \times 10^5$

The increase of values of (n) and (A), for different notch root radius, show that the number of cycles required initiate a fatigue-crack, (N_i), can not only be related to the (ΔK_I) but also related to the notch tip radius.

Barsom and McNicol [4] show that, for HY-130 steel, $n=2$ for fatigue-crack increase to $n=8$ for unnotched specimen.

The data presented in figure-5.2 indicated that the number of cycles required to initiate a fatigue-crack at the tip of the notch, N_i , is related to the parameter $(\Delta K_I / \sqrt{\rho})$. This relation is defined by the equation-

$$N_i = \beta \frac{1}{\left[\frac{\Delta K_I}{\sqrt{\rho}} \right]^k} \quad (4.4)$$

Where, (β) and (k) are constants, for constant notch root radius, the value of (β) can not be predicted in limited fatigue-crack initiation test data. When a small scatter band is plotted for the overall fatigue-crack initiation test data, the value of (β) is varied from $(6.16) \cdot 10^8$ to $(3.16) \cdot 10^9$. The value of exponent (k) is equal to 2.7

It can be noted that $\Delta K_I / \sqrt{\rho}$ increases as N_i increases in figure-5.2. Pearson [1], Jack and Price [2], Barsom and McNicol [4] gave the same relation (4.4) for fatigue-crack initiation.

Pearson suggested that the value exponent (k) was 5 for aluminium alloy, the value of (k) was 4 for mild steel, obtained by Jack and Price.

However, Barsom and McNicol [4] show that the value of exponent (k) is related to the notch root radius (ρ).

If the value of $\Delta K_1 / \sqrt{\rho}$ is equal or lower than 22 kg/mm^2 for 2024-T3 Aluminium alloy, the number of cycles required to initiate a fatigue-crack, N_1 , is greater than 4×10^5 cycles.

In the case of crack-propagation, data of different materials may be combined by normalizing with the elastic modulus (E). The same approach may be tried on initiation data. Hence the value of $\Delta K_1 / \sqrt{\rho}$ is normalized by the elastic modulus (E) and entered in table-2. When the $\log \Delta K_1 / \sqrt{\rho} E$ v.s $\log N_1$ is plotted, it can be seen that the test points of 2024-T3 Aluminium alloy and steel lie on the straight lines in figure-5.3

The slope of lines are;

$k = 3.7$	for	Jack and Price
$k = 4$	for	Barsom and McNicol
$k = 6.2$	for	Vardar
$k = 2.7$	for	2024-T3
$k = 4.82$	for	Pearson

In this study, the test results are in good agreement with Barsom and McNicol, Jack and Price, Pearson. In the low-cycle region, the value of $\Delta K_1 / \sqrt{\rho} E$ is greater than the 3×10^{-3} for steel and aluminium alloy.

An experimental fatigue notch factor which characteristic of both the mechanical notch and material. It is called K_f and defined as the ratio of the fatigue limits of unnotched specimen and a notched specimen during tests of the same type. As it is not possible to carry out a comparison with tests on unnotched specimens when the notched ones are compact tension specimen. This coefficient is determined by means of an empirical formula which is given by Neuber.

$$K_f^N = 1 + \frac{K_T - 1}{1 + \sqrt{A/\rho}} \quad (4.5)$$

$$A^{1/2} = (24 / \sigma_{ult})^3 \text{ in.}^{1/2} \quad (4.6)$$

Where, A is a material constant. Heywood [1] says that for aluminium alloy, $A = 0.07 \text{ mm}$.

Knowing K_f^N , it is possible to calculate in each case the amplitude of the maximum alternating stress at the notch root by the formula,

$$\Delta \sigma_{max} = K_f^N \times \Delta \sigma_{nom} \quad (4.7)$$

In elastic analysis, the parameter K_T , which is defined elastic stress concentration factor, is possible to write as [5]

$$K_T = \frac{1}{\Delta\sigma_{nom}} \times \frac{2\Delta K_I}{\sqrt{\pi\rho}} \quad (4.8)$$

The values of K_T and K_f^N are calculated for each specimen and entered in table - 1

In figure-5.4 $\log K_f^N \times \Delta\sigma_{nom}$ v.s $\log N_i$ is plotted. It can be shown that the number of cycles required to initiate a fatigue-crack is related to $K_f^N \times \Delta\sigma_{nom}$ in log-scale.

Pearson suggested that N_i could be related to $K_f^N \times \Delta\sigma_{nom}$ linearly in log-scales for L 65 aluminium alloy.

CHAPTER - V

CONCLUSION

There are two different points of view on fatigue-crack initiation of the materials under cyclic-loading. One of them elastic-approach the other one is elasto-plastic approach.

In this study, the elastic approach was used and the fatigue-crack initiation was investigated by using linear-elastic-fracture-mechanics (LEFM) concepts and theory of stress-concentration in notched specimens.

The number of cycle required to start a fatigue-crack in the low-cycle region, which is defined $N_i \leq 5 \times 10^4$ cycles, can be calculated by equation-5.1

$$N_i = A (\Delta \sqrt{v_{nom}})^{-n} \quad (5.1)$$

The stress intensity factor fluctuation ΔK_i have been calculated from the equation-4.1 for compact tension specimen. The test results are goodⁱⁿ agreement with Barsom-McNicol, Pearson and Jack-Price. It can be deduced that the number of load cycles required to initiate a fatigue-crack is related to the ratio of the stress-intensity-factor fluctuation to the square root of the notch root radius. This relation is defined by the below formula.

$$N_i = \beta \frac{1}{\left[\frac{\Delta K_i}{\sqrt{\rho}} \right]^k} \quad (5.2)$$

Where, the value of exponent (k) is equal to 2.7

Fatigue-crack initiation can be expressed in terms of the maximum stress fluctuation $\Delta \sigma_{\max}$ at the notch tip, because $\Delta K_i / \sqrt{\rho}$ is related to $\Delta \sigma_{\max}$.

For 2024 - T3 aluminium alloy, if the value of $\Delta K_i / \sqrt{\rho}$ is equal or less than 22 kg/mm^2 , the number of cycles required to initiate a fatigue-crack is more than 4×10^5 cycles. This criterion can be defined as a threshold value for the notched structural components because the fatigue limit of 2024 - T3 aluminium alloy $17 - 20 \text{ kg/mm}^2$ is based on 10^8 cycles.

Normalizing the equation of $\left(\Delta K_i / \sqrt{\rho} \right)_{th} = 22 \text{ kg/mm}^2$ we get;

$$\frac{\Delta K_I}{\sigma_{ys} \sqrt{\rho}} = 0.74 \quad (5.3)$$

Fatigue-crack initiation threshold in aluminium alloys of various yield strengths can be predicted by using equation- Barson and McNicol suggested that threshold value of $\Delta K_I / \sigma_{ys} \sqrt{\rho}$ were 0.6 for various steels.

When the $\log \Delta K_I / E \sqrt{\rho}$ v.s $\log N_i$ is plotted for steels and aluminium alloys, it can be seen that the test results lie on the different straight lines for different materials and there is not any test point below $\Delta K_I / E \sqrt{\rho} = 3 \times 10^{-3}$ in low-cycle region.

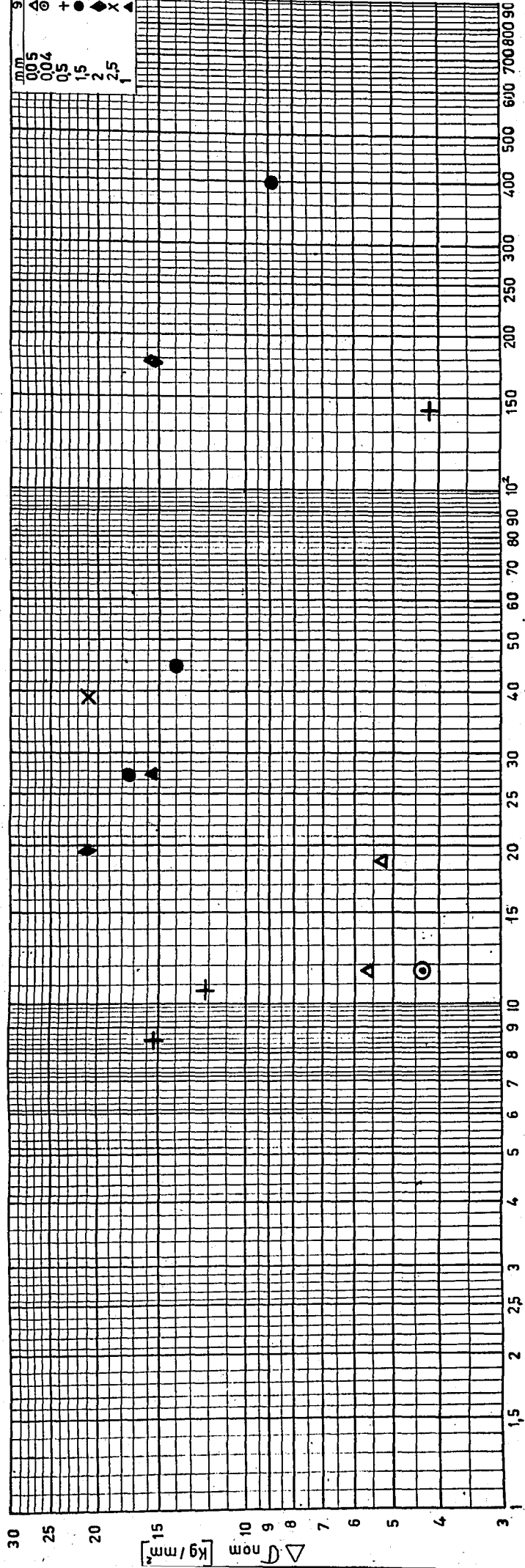
If the notch factor is known K_f , fatigue-crack initiation life can be predicted in terms of the maximum alternating stress at the notch tip in elastic analysis. It is difficult to define the material constant (A'). ($\Delta \sigma$) and ($\Delta \epsilon$) which are calculated using finite element methods or by using the cyclic stress-strain curve and Manson-Coffin one for each N_i in elasto-plastic analysis. K_f and K_f^P parameters do not yield same accuracy for the prediction of the number of cycles N_i in terms of the parameter $\Delta K_I / \sqrt{\rho}$.

TABLE - I

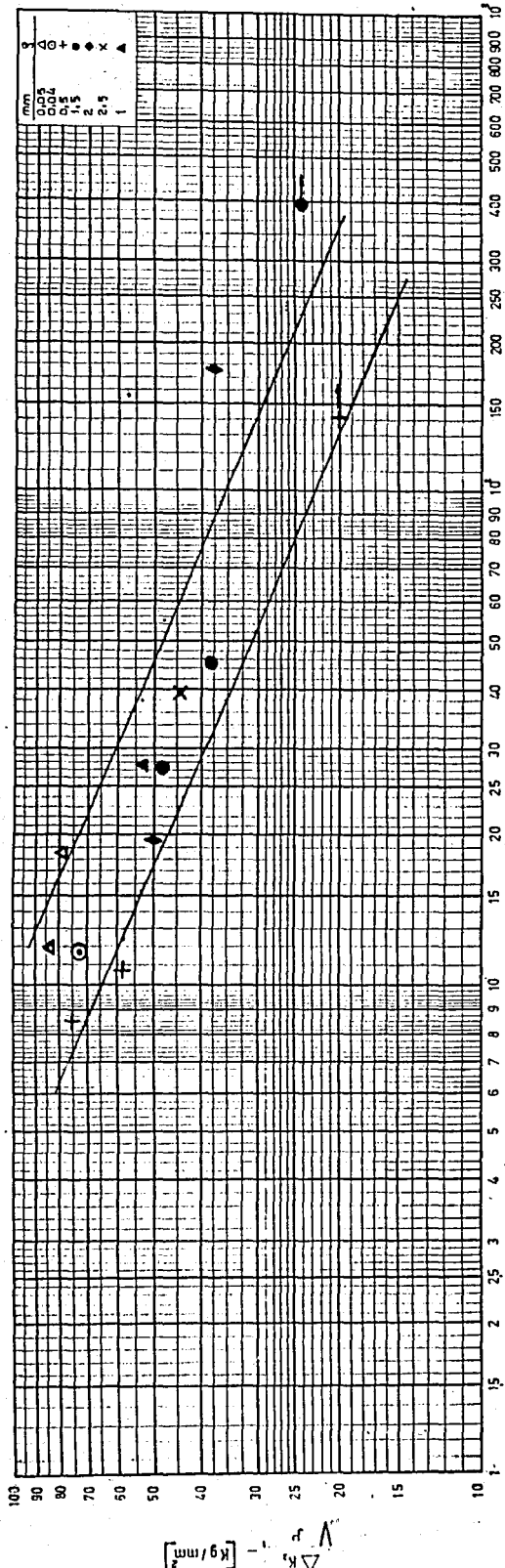
SPECIMEN No.	ROOT RADIUS (mm)	LOAD ΔP (kg)	$\Delta K_{I, 3/2}$ (kg/mm ^{3/2})	$\Delta K_I / \sqrt{P}$ (kg/mm ²)	$\Delta \sigma_{max}^N$ kg/mm ²	$\Delta \sigma_{max}$ kg/mm ²	$\Delta \sigma_{nom}$ kg/mm ²	K_t	K_f^N	N_i (cycles)
2	0.05	160	18.88	84.44	46.40	95.28	5.6	17.014	8.34	11930
3	0.05	150	17.68	79.07	46.1	89.92	5.25	16.99	8.78	18800
4	0.04	126	14.85	74.28	38.58	83.82	4.41	19	8.75	11750
8	0.5	350	41.3	58.40	51.3	65.9	12.25	5.38	4.187	10710
9	0.5	120	14.5	20	17.57	22.58	4.2	5.37	4.185	140510
10	0.5	450	53.1	75.10	53.39	67.61	15.75	4.29	3.39	8600
12	1	450	53.1	53.1	50.62	59.91	15.75	3.8	3.214	27750
13	1.5	250	29.5	24.09	23.89	27.18	8.75	3.106	2.731	40000
14	1.5	500	59	48.18	47.79	54.36	17.5	3.106	2.731	27600
15	1.5	40	47.2	38.53	38.23	43.38	14	3.106	2.731	45450
18	2	600	70.8	50.06	50.88	56.49	21	2.69	2.423	19450
19	2	450	53.1	37.55	38.16	42.37	15.75	2.69	2.423	178910
21	2.5	600	70.8	44.77	46.26	50.52	21	2.405	2.203	39750

TABLE - II

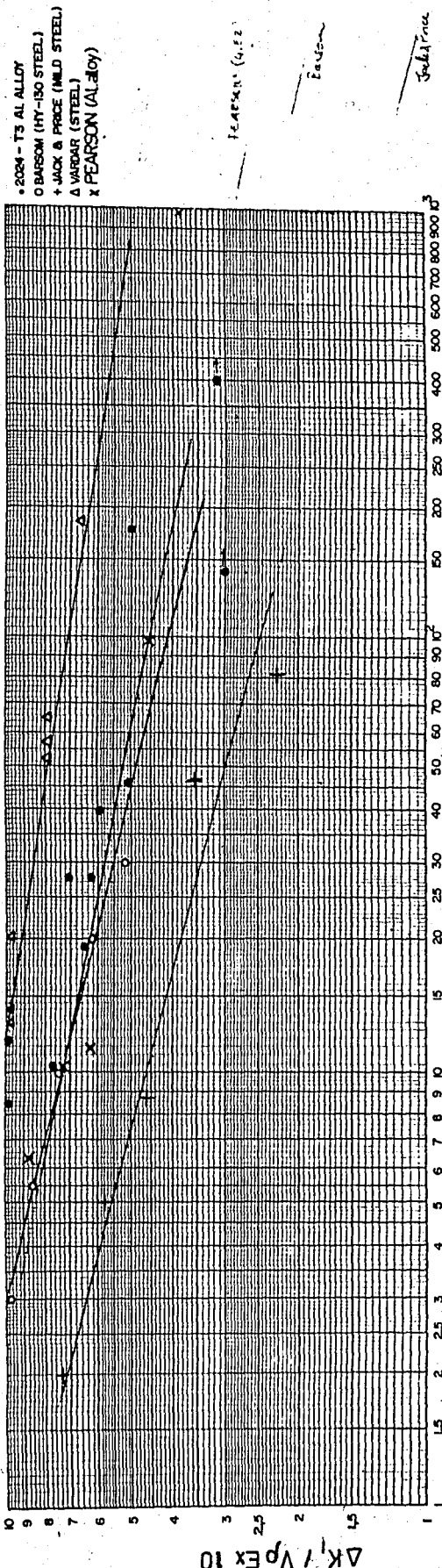
	$\Delta K/\sqrt{P}$	$\Delta K/\sqrt{P}$	Ni
BARSON And MCNICOL	120	$5.7 \cdot 10^{-3}$	30 000
	132	$6.3 \cdot 10^{-3}$	20 000
	160	$7.6 \cdot 10^{-3}$	10 000
	108	$8.57 \cdot 10^{-3}$	5 500
	208	$9.9 \cdot 10^{-3}$	3 000
JACK And PRICE	47.1	$2.24 \cdot 10^{-3}$	81750
	73.84	$3.52 \cdot 10^{-3}$	46486
	97.04	$4.62 \cdot 10^{-3}$	8720
	123	$5.86 \cdot 10^{-3}$	5000
	154.7	$7.36 \cdot 10^{-3}$	2000
VARDAR	143	$6.80 \cdot 10^{-3}$	157 000
	165	$7.85 \cdot 10^{-3}$	52 000
	165	$7.85 \cdot 10^{-3}$	57 000
	165	$7.85 \cdot 10^{-3}$	65 000
	208	$9.9 \cdot 10^{-3}$	13 000
	208	$9.9 \cdot 10^{-3}$	14 000
	208	$9.9 \cdot 10^{-3}$	20 130
	208	$9.9 \cdot 10^{-3}$	14 000
PEARSON	42.7	$3.85 \cdot 10^{-3}$	10^6
	50	$4.55 \cdot 10^{-3}$	98 000
	54.9	$6.3 \cdot 10^{-3}$	11 300
	67.6	$7.35 \cdot 10^{-3}$	10 250
	95.5	$8.78 \cdot 10^{-3}$	6 400



Ni x 10³
 FIGURE -5.1



Nix10^3
 FIGURE - 5.2



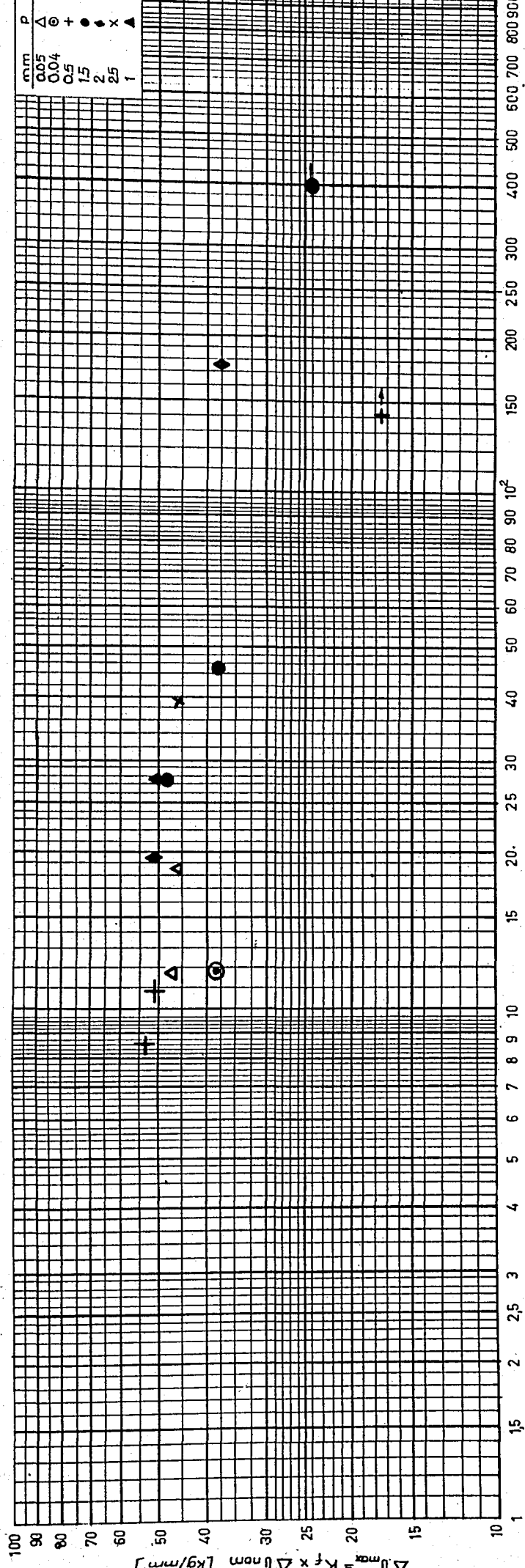


FIGURE-5.4

REFERENCES

1. PEARSON, S.

Fatigue-crack initiation and propagation in half inch thick specimens of aluminium alloy".

R.A.E. technical report 71109, May 1971

2. JACK, A.R. and PRICE, A.T.

"The initiation of fatigue cracks from notches in mild steel plates"

International Journal of fracture mechanics Vol.6, No 4
Dec. 1970

3. KIM, Y. MURA, T. and FINE, M.E.

"Fatigue-crack initiation and microcrack growth in 4140 Steel"

American society for metals and metallurgical society of AIME. Vol.96, pp 1679-1683 Nov. 1978

4. BARSOM, J.M and McNICOL, R.C

"Effect of stress concentration on fatigue-crack initiation in HY-130 steel".

ASTM STP 559, pp 183-204

5. BAUS, A. LIEURADE, H.P. SANZ, G and TURCHON, M.

"Corralation between fatigue-crack initiation at the root of a notch and low-cycle fatigue data".

ASTM STP 631, pp 97-111, 1977

6. SAANOUNI, K and BATHIAS, C.
"Study of fatigue-crack initiation in the vicinity of notches"
Engineering fracture mechanics, Vol.16, No 5, pp 695-732, 1982
7. VARDAR, Öktem
"Akma sınırı ötesinde yorulma çatlakları ilerlemesi"
Doçentlik tezi, Boğaziçi Üniversitesi, İstanbul, Eylül 1980
8. ROLFE and BARSOM
"Fracture and fatigue control in structures"
Application of fracture mechanics. Prentice-Hall Inc.
Englewood Cliff. New Jersey 1977
9. KNOTT, J.F.
"Fundamentals of fracture mechanics"
Butterworth and Co.Ltd. London 1973
10. POPE, J.A.
"Metal Fatigue"
Chapman-Hall Ltd. 1959
11. Mc Clinckton, F.A. and ARGON, A.S.
"Mechanical behavior of Materials", Addison-Westey
publishing Comp. Inc. 1966
12. MARIN, J.
"Mechanical behavior of engineering materials"
Prentice-Hall Inc. Englewood Cliffs.N.J 1963

13. YOKOBORI, T.

"The strength, fracture and fatigue of materials"

P.Noodhof Ltd. Groningen - 1964

14. SANDOR, B.I

"Fundamentals of cyclic-stress and strain"

The university of Wisconsin Press, 1977

15. Metals Handbook "Properties and selection of Metals"

8 th edition Vol.1 American society for Metals,

pp. 938-941, Metals park Ohio, 1971.